



Fabrication of high-quality nanobeam photonic crystal cavities in 4H silicon carbide with embedded color centers

Citation

Brachera, David O., and Evelyn L. Hua. 2016. "Fabrication of high-quality nanobeam photonic crystal cavities in 4H silicon carbide with embedded color centers." In Proc. of SPIE Vol, vol. 9762, pp. 97620Z-1. doi:10.1117/12.2211230

Published Version

doi:10.1117/12.2211230

Permanent link

<http://nrs.harvard.edu/urn-3:HUL.InstRepos:34216538>

Terms of Use

This article was downloaded from Harvard University's DASH repository, and is made available under the terms and conditions applicable to Other Posted Material, as set forth at <http://nrs.harvard.edu/urn-3:HUL.InstRepos:dash.current.terms-of-use#LAA>

Share Your Story

The Harvard community has made this article openly available.
Please share how this access benefits you. [Submit a story](#).

[Accessibility](#)

Fabrication of high-quality nanobeam photonic crystal cavities in 4H silicon carbide with embedded color centers

David O. Bracher^{a,*}, Evelyn L. Hu^a

^aJohn A. Paulson School of Engineering and Applied Sciences, Harvard Univ., Cambridge, MA 02138

ABSTRACT

A wide band-gap semiconductor with a long history of growth and device fabrication, silicon carbide (SiC) has attracted recent attention for hosting several defects with properties similar to the nitrogen vacancy center in diamond. In the 4H polytype, these include the silicon vacancy center and the neutral divacancy, which have zero phonon lines (ZPL) in the near-IR and may be useful for quantum information and nanoscale sensing. For many such applications, it is critical to increase the defect emission into the ZPL by coupling the emission to an optical cavity. Accordingly, we have pursued the fabrication of high quality 1D nanobeam photonic crystal cavities (PCCs) in 4H-SiC, using homoepitaxially grown material and a photoelectrochemical etch to provide optical isolation. These PCCs are distinctive in their high theoretical quality factors ($Q > 10^6$) and low modal volumes ($V < 0.5 (\lambda/n)^3$). Here, we present arrays of nanobeam PCCs with varied lattice constant containing embedded silicon vacancy defects generated by electron irradiation, to assess its viability as a method for defect creation. The lattice constant variation allows us to create devices with modes spanning the entire range of the silicon vacancy emission. We accordingly demonstrate nanobeam PCCs with resonant modes near both ZPLs of the silicon vacancy defect. Moreover, we measure devices with the highest Q cavity modes coupled to point defect emission in SiC yet reported, providing evidence that electron irradiation can be used to generate point defects while maintaining high quality optical devices.

Keywords: silicon carbide, nanobeam photonic crystal cavity, point defects, cavity-emitter coupling

INTRODUCTION

Silicon carbide (SiC) is a wide band-gap semiconductor with an extensive history of research in fields spanning optoelectronic devices, high-temperature electronics, and micro-electro-mechanical systems^{1,2}. Given this background, SiC has well-developed, robust protocols for growth, doping, and fabrication^{1,2}. These properties make it an excellent platform for the fabrication and study of nanoscale devices.

Moreover, given recent interest in the nitrogen vacancy (NV) center in diamond, SiC was identified as another potential host of spin-active point defects³. Indeed, such defects were found in several SiC polytypes⁴, which correspond to different possible crystal lattice arrangements. In particular, the 4H-SiC polytype hosts both divacancy defects⁵ with photoluminescence (PL) emission ranging from 1070-1300 nm and silicon vacancy defects⁶⁻⁸ with PL emission spanning 860-1100 nm. Like the diamond NV center, the level structure of these defects allows their spin state to be read out through optically detected magnetic resonance (ODMR). The defects also show long spin coherence lifetimes^{5,6}. Therefore, these defects are excellent candidates for solid-state quantum information^{3-5,9,10} as well as quantum sensing of magnetic fields¹¹, electric fields¹², and temperature¹¹.

However, only a small fraction of the fluorescence of these defects is emitted into their zero phonon lines (ZPL), while the majority is emitted into the accompanying phonon sideband. For many protocols in quantum information and sensing, only light emitted into the ZPL can be used. Therefore, it is of great importance to modify the defect emission to increase the fraction of ZPL emission¹³. A primary way to achieve this goal is through the coupling of the defects to an optical cavity, as has been accomplished with the diamond NV center¹⁴⁻¹⁷. In order to maximize coupling (and therefore the increase in ZPL emission), a cavity must have a high quality factor (Q) and a small modal volume (V), its resonant mode must spectrally overlap the defect ZPL, and the electric field of the resonant mode must spatially overlap the position of the defect¹⁴.

*dbracher@fas.harvard.edu

Given the presence of spin-active defects with excellent characteristics in addition to well-developed fabrication procedures, 4H-SiC is thus a promising platform for developing solid-state defects coupled to optical cavities. However, it is important to understand not only how to create high quality optical cavities in this material (to maximize cavity-defect coupling) but also how to do so while incorporating the desired defects. In previous work¹⁸, we have demonstrated the fabrication of 1D photonic crystal cavities (PCC) in 4H-SiC with high measured values of Q. Additionally, we have observed coupling of the PCC resonant modes to the emission of silicon vacancy defects that were created through C₁₂ ion implantation. In this work, we instead study arrays of nanobeam PCCs in 4H-SiC coupled to silicon vacancy defects generated through electron irradiation. Electron irradiation was used as an alternative to ion implantation because, while ion implantation can create defects at a targeted depth, bombardment with high energy ions can potentially be damaging to the implanted material¹⁹. Maintaining high material quality is important to preserve the spin properties of the defects as well as to ensure high quality optical devices. Thus, it is worthwhile to study electron irradiation as a possible alternative for defect generation in photonic cavities. The arrays fabricated in this work consist of nanobeam PCCs with varied lattice spacing. This variation allows us to demonstrate the effects of changing the PCC dimensions and accordingly to fabricate beams with resonant modes spanning a wide range of wavelengths. We are thereby able to fine tune the fabrication by determining what lattice constants are ideal for coupling to specific defect species. Indeed, here we demonstrate cavities with modes very close in wavelength to both silicon vacancy ZPLs. Additionally, we report the highest Q devices coupled to point defect emission in SiC, showing that electron irradiation may be a viable method for defect generation in high quality optical cavities.

METHODS

To fabricate photonic cavities in 4H-SiC, we begin with an n-type 4H-SiC substrate (nitrogen, 10^{19} cm^{-3}) onto which a p-type epilayer (aluminum, 10^{17} cm^{-3} , Norstel AB) is homoepitaxially grown. The epilayer has a thickness of 250 nm and serves as the device layer, whereas the underlying substrate is eventually etched away to provide the optical isolation necessary to produce confined cavity modes. This wafer is diced into small pieces (6mm to a side) that can then be used to fabricate the desired devices. Using electron beam evaporation, we deposit 100 nm of nickel on the n-type side of our samples to serve as a contact. The samples are annealed post-deposition to improve the metal's adhesion. Finally, we evaporate 110 nm of aluminum on the p-type surface as an etch mask for the SiC.

Having prepared the samples in this manner, we use electron beam lithography to define our selected device design in positive-tone resist (PMMA C6), as shown in figure 1a. This pattern is transferred by means of a chlorine-based inductively-coupled reactive ion etch (ICP-RIE) to the aluminum hard mask and then to the SiC by a further fluorine-based ICP-RIE step (fig. 1b). The SiC must be etched deeply enough to expose both the epilayer and the amount of n-type substrate needed to be removed for proper optical isolation (here, at least 650 nm).

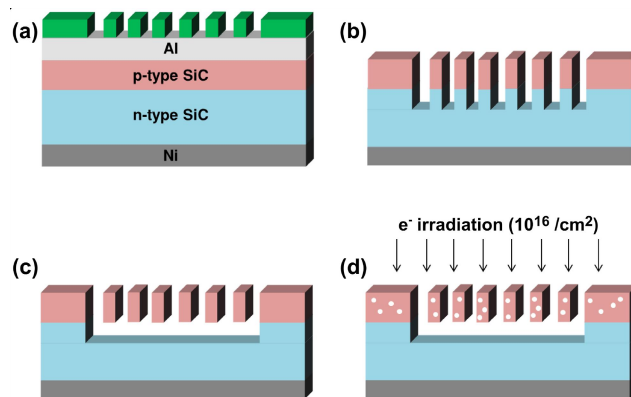


Figure 1. Procedure to fabricate PCCs in 4H-SiC. (a) Epilayer of p-type SiC grown on n-type substrate, with nickel contact deposited on substrate and aluminum hard mask on epilayer. Device pattern defined by electron beam lithography with PMMA resist. (b) Pattern is transferred to aluminum mask and then to SiC epilayer and substrate. (c) Dopant-selective photoelectrochemical etch removes n-type material beneath patterned device. (d) Post-fabrication, devices undergo electron irradiation at a dosage of 10^{16} cm^{-2} to create silicon vacancy defects (schematically indicated by white dots).

After the pattern has been transferred into the SiC, a dopant-selective photoelectrochemical (PEC) etch^{18, 20} is used to remove the n-type substrate beneath the etched devices, while the p-type device layer is left untouched (fig. 1c.). During this etch, the device is submerged in 0.2 M KOH with a potential of 0.2 V applied while illuminated by a 120 W mercury lamp shortpass filtered at 500 nm. In the n-type substrate, photo-generated holes are swept to the surface where they participate in a dissolution reaction of the SiC. Holes in the p-type substrate are swept away from the surface, and therefore no etching takes place. This method of undercutting the PCC devices was chosen in order to be able to use high-quality, epitaxially grown material, as opposed to the ion-damaged, wafer-bonded material as used in, for example, the SmartCut method²¹. High quality material is important for preserving the quality of the devices as well as the properties of the defects, and indeed we have demonstrated high quality PCCs with this method¹⁸.

Once the devices have been patterned, we generate silicon vacancy defects using irradiation by 2 MeV electrons (Roberto Uribe, Kent State) at a dose of 10^{16} cm^{-2} with no post-annealing (fig. 1d). The irradiation creates vacancies throughout both the epilayer and the underlying substrate; however, as there is significant isolation between the device layer and the substrate after the PEC etch, only the defects in the epilayer are of concern. The 10^{16} cm^{-2} dose was chosen to be high enough to create a homogeneous concentration of defects throughout the material, as opposed to single, isolated defects^{22, 23}. This way we could be assured that the PCCs would nearly all be coupled to the defects—at this dose we expect on the order of 20 defects within the cavity field region (fig. 2a inset, see below)⁷. Additionally, we did not irradiate at higher doses in order to prevent possible lattice damage that can appear at very large doses.

The precise design chosen for our optical cavities was a 1-D nanobeam PCC²⁴. This design (fig. 2a) consists of a periodic array of holes in one dimension. The outer regions have constant lattice spacing between the holes and constant hole size. They function as Bragg mirrors. In the inner region, the lattice constant is linearly tapered to 84% of its original size, as is the size of the holes. This linear tapering gradually confines the light within the inner cavity region, which leads to higher theoretical Q by eliminating cavity electric field Fourier components within the light cone²⁵.

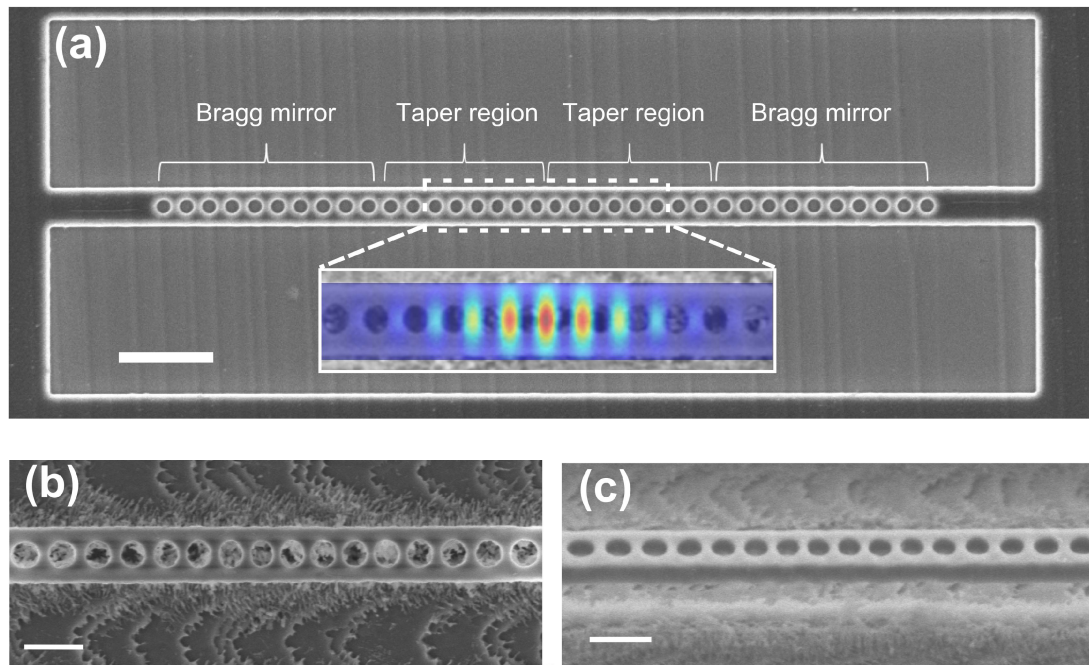


Figure 2. Nanobeam PCC design and SEM micrographs. (a) SEM micrograph of full PCC design showing the outer Bragg mirror regions with constant hole size and spacing, as well as inner regions where spacing and hole size are linearly tapered. Scale bar indicates 1 μm . Inset shows simulated electric field profile of fundamental TE mode. (b),(c) SEM micrographs showing top-down and side-angle view of inner, taper region. The elliptical character of the inner holes is clearly visible. Mottling of n-type surface below substrate is an effect of PEC etch. Scale bars indicate 500 nm.

Based on previous investigation of several different nanobeam PCC designs¹⁸, we chose to use a design where the Bragg mirror regions consist of 10 holes on each side, and the inner taper regions consist of 8 holes on each side of the beam center. Moreover, the tapering of the hole size is done only in the direction parallel to the beam axis, creating ellipses. The inset of figure 2a shows the simulated electric field profile of the fundamental TE mode (Lumerical Inc.). Figures 2b and 2c show SEM micrographs of this inner region. The increasing elliptical character of the holes as they become closer to the center is clearly visible. The mottling of the underlying n-type substrate is an effect of the PEC etch and does not affect device quality. The theoretical Q of this design is $\sim 5 \times 10^6$, with a modal volume of $\sim 0.4 (\lambda/n)^3$.

RESULTS

We begin by characterizing the effect of varying the lattice spacing of the fabricated nanobeam PCCs. Figure 3a shows an array of PCCs, with lattice spacings, a , varying from 240 to 310 nm in 10 nm increments. As the lattice spacing increases, so should the wavelengths of the resonant modes. This range of spacings was chosen on the basis of FDTD simulations (Lumerical Inc.) to achieve resonant modes in the range of 750-1000 nm, given that the silicon vacancy luminescence spans ~ 860 -1100 nm, with ZPLs at 859 nm (V_1) and 916.5 nm (V_2). The presence of two ZPLs is due to the two possible orientations of the defect within the lattice. Fabricating these arrays thus enables us to determine what cavity dimensions will be ideal for having resonant modes near the defect ZPLs. Indeed, used in conjunction with methods of spectrally tuning the PCC resonant modes¹⁸, the arrays should allow for a high degree of success in eventually bringing PCC modes in resonance with the defect ZPLs.

We first acquired PL spectra of the nanobeam PCCs before they had been electron irradiated (fig. 3b). Measurements were done in a commercially available Raman spectrometer (Horiba Jovin Yvon Inc.). The spectra were taken with an excitation laser of 532 nm operating at ~ 3 mW. Resonant PCC modes can be seen decorating a visible background luminescence ranging from ~ 600 -800 nm, intrinsic to the material¹⁸. These measurements confirmed that the PCCs are well behaved: most devices exhibited 2-4 resonant modes, and a gradual red-shift in the modes was observed as the lattice spacing increased, as expected. Additionally, in devices with lattice spacing of greater than 280 nm, no modes were seen observed, as the modes were likely at too high of wavelengths to couple to the available luminescence

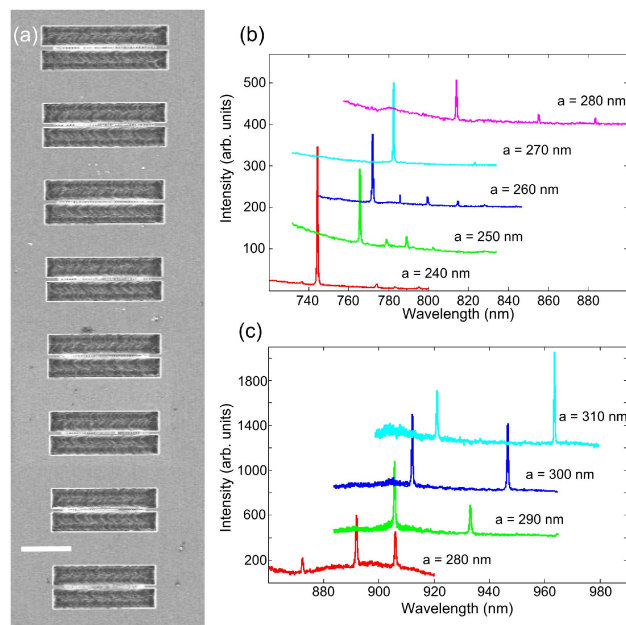


Figure 3. Nanobeam PCC array micrograph and PL spectra. (a) SEM micrograph of array of 9 nanobeam PCCs, with lattice spacing, a , ranging from 240-310 nm in increments of 10 nm. Scale bar indicates 5 μm . (b) PL spectra of PCCs with smaller lattice spacing before electron beam irradiation with an excitation wavelength of 532 nm. Modes decorate intrinsic visible background luminescence. (c) PL spectra of PCCs with larger lattice spacing pumped at an excitation wavelength of 760 nm. Modes decorate silicon vacancy defect luminescence.

After electron irradiation, we once again acquired PL spectra of the nanobeam PCCs (fig. 3c). The spectra were taken in a home-built setup using a Ti:Sapphire laser tuned to 760 nm at a power of 5 mW. As before, most PCCs showed 2-4 resonant modes, and a gradual red-shift of the modes was observed as the PCC lattice spacing increased. In devices with lattice spacings greater than 280 nm that had previously not displayed modes, modes were now visible, decorating the silicon vacancy defect luminescence. In PCCs with 280 nm lattice spacing, the longer wavelength modes observed before irradiation also became more prominent as they now coupled to the silicon vacancy luminescence. Devices with lattice spacing below 280 nm did not show any modes coupled to the silicon vacancy defects.

These results illustrate the close relationship between optical cavities and embedded emitters to which they are coupled. Just as the cavities allow us to better study emitters within, the presence of the emitters also allows us to study cavities with modes that were previously invisible. To better characterize the observed resonant modes coupled to the silicon vacancy defects, we analyzed spectra of the nanobeam PCCs with lattice spacings of 290, 300, and 310 nm in ~15 arrays. While there is some variation among devices of the same lattice spacing, the modes could be seen to be grouped into 3 prominent sets, each of which exhibits a red-shift as the lattice spacing increases. The results are summarized in table 1, which shows both the mean wavelength of the 3 groups for each lattice spacing, as well as the standard deviation of each group (typically ~5-10 nm). Groups 1 and 2 are prominently seen in fig. 3c. The modes in group 1 are important in that they are typically very close in wavelength to the V_2 ZPL in devices with 300 nm and 310 nm lattice spacings. Additionally, the second group of modes corresponds fairly well to simulated values for the wavelength of the primary TE cavity mode, and the third group corresponds to a higher order mode also typically seen in simulations. Other modes may be due to different mode orders or polarizations.

Table 1. Mean wavelengths and standard deviations of 3 mode groupings observed in nanobeam PCCs

Lattice spacing	Mode 1 λ (std.), nm	Mode 2 λ (std.), nm	Mode 3 λ (std.), nm
290 nm	902.9 (8.7)	930.9 (5.0)	958.1 (6.7)
300 nm	915.5 (7.9)	947.6 (6.5)	986.6 (7.4)
310 nm	921.4 (13.3)	961.7 (8.2)	1006.6 (9.9)

In addition to the three groups of modes analyzed above, some PCCs with lattice spacings of 300 nm and 310 nm exhibit resonant modes at wavelengths below 880 nm. These devices are thus of great interest in that they show modes near both ZPLs of the silicon vacancy defect—the lower wavelength modes near the V_1 ZPL at 859 nm and the modes in group 1 with wavelengths near the V_2 ZPL at 916.5 nm. To examine the proximity of these modes to the defect ZPLs and to further confirm that the devices are indeed coupled to the silicon vacancy defects, we measure the low temperature PL spectra of two such PCCs. The room temperature PL spectra of the two selected devices is seen in fig. 4a,b. The spectra were again obtained by pumping with the Ti:Saph laser tuned to 760 nm at 5 mW of power. As expected, there are no visible ZPLs within the spectra—only the resonant modes are seen decorating the silicon vacancy sideband luminescence. The two modes of the device in fig. 4a (lattice spacing 300 nm) show Q of 2,500 (877 nm) and 3,100 (912.5 nm), and the modes of the device in fig. 4b show Q of 1,900 (863 nm) and 2,500 (921 nm).

The devices were then cooled to 77 K with liquid nitrogen in a continuous flow cryostat (Janis). Upon cooling, both the V_1 and V_2 (less prominent than V_1) ZPLs become clearly visible in the spectra (fig 4c, d), confirming that the nanobeam PCCs are indeed coupled to the silicon vacancy defects. Furthermore, given the proximity of the resonances to the ZPLs in both devices, they are ideal candidates to be tuned into spectral overlap with the ZPLs. The cavity resonances in the device shown in fig. 4b,d are both similarly red-shifted from the ZPLs and therefore could potentially be tuned using previously reported methods¹⁸ into simultaneous resonance with both ZPLs. On other hand, the device shown in fig. 4a,c could be similarly blue shifted so that the lower wavelength mode overlaps the V_1 ZPL or could be red shifted using gas condensation tuning so that the longer wavelength mode matches the V_2 ZPL. Such experiments will be the goal of future work.

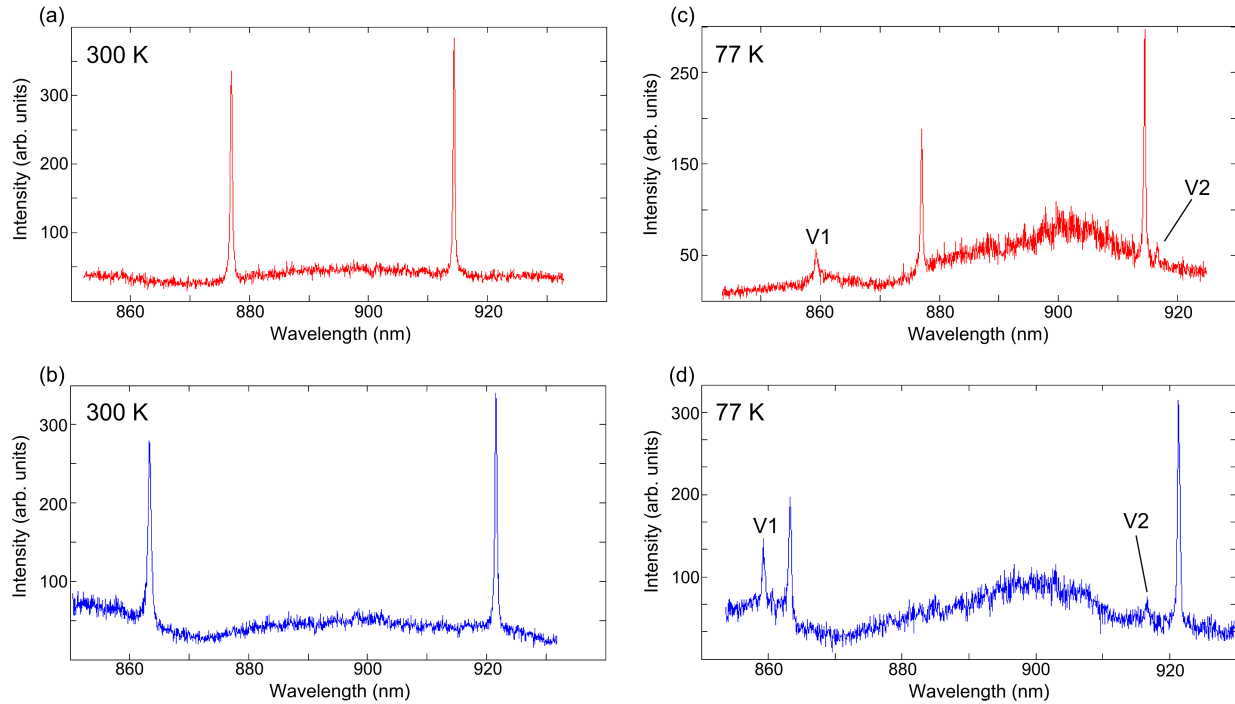


Figure 4. PL spectra of nanobeam PCCs with resonances near silicon vacancy ZPLs. (a),(b) Room temperature spectra for two different devices. Device shown in (a) has a 300 nm lattice spacing and modes with Q of 2,500 (877 nm) and 3,100 (912.5 nm). Device shown in (b) has 310 nm lattice spacing and modes with Q of 1,900 (863 nm) and 2,500 (921 nm). (c),(d) Spectra of devices shown in (a) and (b), respectively, cooled to 77 K. At this temperature, silicon vacancy ZPLs become visible near resonant modes.

Finally, we report on the high measured Q factors of the devices fabricated in this work. In previous work¹⁸, the majority of measured devices coupled to the silicon vacancy emission showed Q on the order of 700-1,300, with no devices showing Q above 2,000. Moreover, the intensity of resonant modes was not very high with respect to the defect luminescence they decorated (2-4x defect emission). This low intensity indicates that the cavities are not enhancing the defect emission very well, likely due to the modest Q of the devices.

On the other hand, in the devices studied here, more than half of the PCCs coupled to silicon vacancy defects showed modes with $Q > 2,000$, with many showing modes with Q between 2,500 and 4,000. Figure 5 shows the PL spectra of a few representative examples of these high quality devices coupled to silicon vacancy luminescence. The inset of each subfigure shows a Lorentzian fit to the mode inside the dashed box. The device shown in fig. 5d has the highest Q (4,100, ~ 230 pm full width at half maximum) of any optical cavity coupled to a point defect in SiC measured to date. Additionally, the resonant modes of many devices show high intensity with respect to the defect luminescence (10-20x), likely indicative of a good degree of luminescence enhancement. Indeed, the high measured Q factors across dozens of PCCs as well as the large mode intensities observed suggest that creation of defects through electron irradiation of fabricated devices is a promising way to create high quality optical devices coupled to defect centers in SiC.

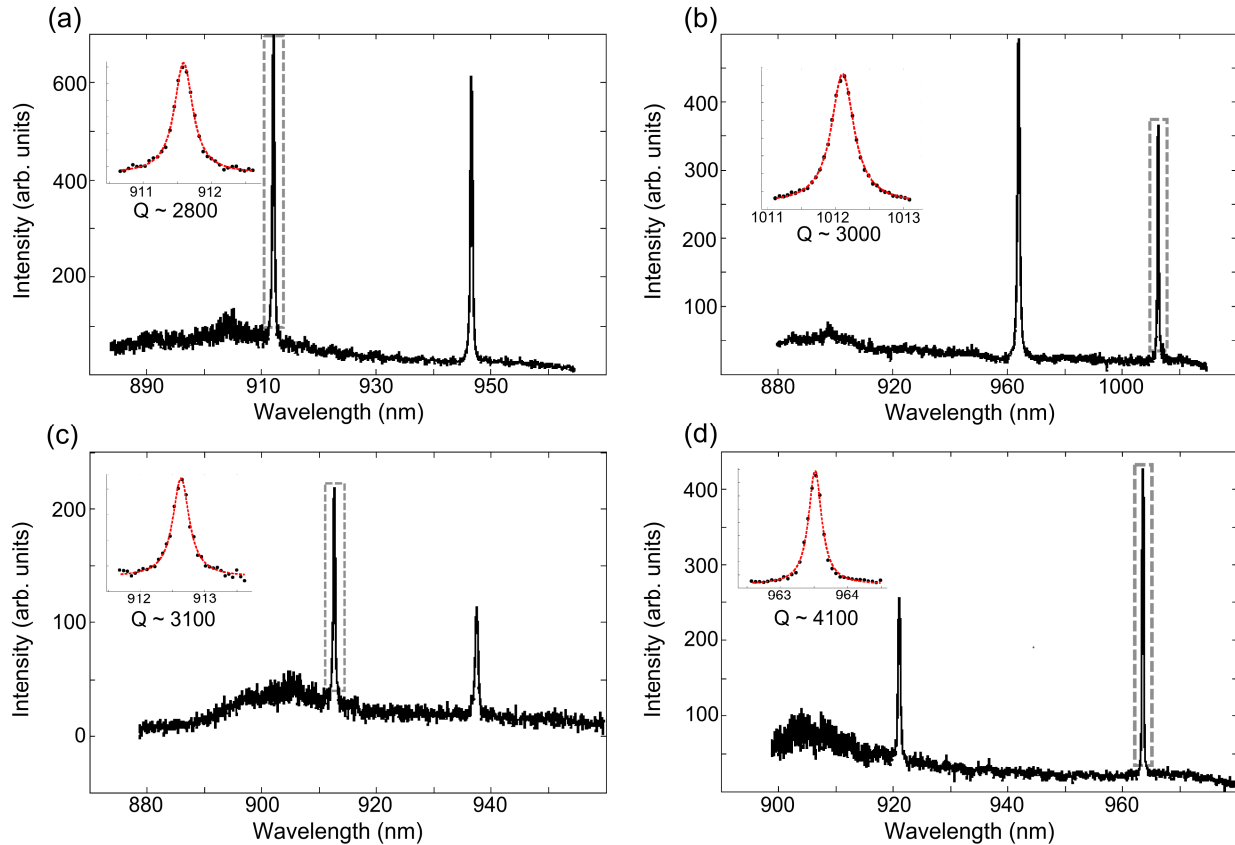


Figure 5. PL spectra of high Q nanobeam PCC modes. Devices are pumped by Ti:Saph laser tuned to 760 nm. Insets show Lorentzian fits to modes outlined in dashed boxes.

4. CONCLUSIONS

We have demonstrated arrays of nanobeam PCCs in 4H-SiC coupled to silicon vacancy defects generated by electron irradiation to investigate its utility as a method of creating defects in high quality optical cavities. We have also investigated the effect of varying the PCC lattice spacing and determined the optimal range for coupling to silicon vacancy defects. Accordingly, we have measured devices with high Q resonant modes in close spectral proximity to the silicon vacancy ZPLs, and we have demonstrated cavities with the highest measured Q coupled to point defects in SiC to date. These results show the promise of using electron irradiation to generate point defects while maintaining high quality optical devices. Future work will include tuning resonant modes into overlap with the ZPLs to seek Purcell enhancement of the defects. Additionally, we will do further analysis of nanobeam PCCs with defects generated both through ion implantation and electron irradiation to fully characterize any potential differences in device quality as well as to compare the defect properties (e.g. spin coherence).

ACKNOWLEDGEMENTS

The authors acknowledge funding from the Air Force Office of Scientific Research, under the QUMPASS program (Award No. FA9550-12-1-0004). This work was performed in part at the Center for Nanoscale Systems (CNS), a member of the National Nanotechnology Infrastructure Network (NNIN), which is supported by the National Science Foundation under NSF award no. ECS-0335765. CNS is part of Harvard University.

REFERENCES

- [1] Choyke, W.J., Matsunami, H. and Pensl, G., [Silicon Carbide: Recent Major Advances], Springer-Verlag Berlin Heidelberg, New York, (2004).

- [2] Sadow, S.E. and Agarwal, A., [Advances in Silicon Carbide Processing and Applications], Artech House, Inc., Norwood, (2004).
- [3] Weber, J. R., Koehl W. F., Varley, J. B., Janotti, A., Buckley B. B., Van de Walle, C. G. and Awschalom, D. D., "Quantum computing with defects," *Proc. Natl. Acad. Sci.* 107(19), 8513-8518 (2010).
- [4] Falk, A. L., Buckley, B. B., Calusine, G., Koehl, W. F., Dobrovitski, V. V., Politi, A., Zorman C. A., Feng P. X.-L. and Awschalom, D. D., "Polytype control of spin qubits in silicon carbide," *Nat. Commun.* 4, 1819 (2013).
- [5] Koehl, W. F., Buckley, B. B., Heremans, F. J., Calusine, G. and Awschalom, D. D., "Room temperature coherent control of defect spin qubits in silicon carbide," *Nature* 479, 84-87 (2011).
- [6] Widmann, M., Lee, S. Y., Rendler, T., Son, N. T., Fedder, H., Paik, S., Yang L.-P., Zhao N., Yang S., Booker I., Denisenko A., Jamali M., Momenzadeh S. A., Gerhardt I., Ohshima T., Gali A., Janzen E. and Wrachtrup, J., "Coherent control of single spins in silicon carbide at room temperature," *Nat. Mat.* 14, 164-168 (2015).
- [7] Hain, T.C., Fuchs, F., Soltamov, V. A., Baranov, P. G., Astakhov G. V., Hertel, T. and Dyakonov, V., "Excitation and recombination dynamics of vacancy-related spin centers in silicon carbide," *J. Appl. Phys.* 115, 133508 (2014).
- [8] Carter, S. G., Soykal, O. O., Dev, P., Economou, S. E. and Glaser, E. R., "Spin coherence and echo modulation of the silicon vacancy in 4H-SiC at room temperature," *Phys. Rev. B* 92, 161202(R) (2015).
- [9] Falk, A. L., Klimov P. V., Ivady, V., Szasz K., Christle, D. J., Koehl, W. F., Gali, A. and Awschalom D. D., "Optical polarization of nuclear spins in silicon carbide," *Phys. Rev. Lett.* 114, 247603 (2015).
- [10] Klimov, P. V., Falk, A. L., Christle D. J., Dobrovitski, V. V. and Awschalom D. D., "Quantum entanglement at ambient conditions in a macroscopic solid-state spin ensemble," *Sci. Adv.* 1(10), e1501015 (2015).
- [11] Kraus, H., Soltamov, V. A., Fuchs, F., Simin, D., Sperlich, A., Baranov, P.G., Astakhov, G. V. and Dyakonov, V., "Magnetic field and temperature sensing with atomic-scale spin defects in silicon carbide," *Sci. Reports* 4, 5303 (2014).
- [12] Falk, A. L., Klimov, P. V., Buckley B. B., Ivady V., Abrikosov, I. A., Calusine G., Koehl W. F., Gali, A. and Awschalom D. D., "Electrically and mechanically tunable electron spins in silicon carbide color centers," *Phys. Rev. Lett.* 112, 187601 (2014).
- [13] Aharonovich, I. and Neu, E., "Diamond Nanophotonics," *Adv. Opt. Mat.* 2(1), 911-928 (2014).
- [14] Faraon, A., Santori, C., Huang, Z., Acosta, V. M. and Beausoleil R.G., "Coupling of nitrogen-vacancy centers to photonic crystal cavities in monocrystalline diamond," *Phys. Rev. Lett.* 109, 033604 (2012).
- [15] Hausmann, B. J. M., Shields, B. J., Quan, Q., Chu, Y., de Leon, N. P., Evans, R., Burek, M. J., Zibrov, A. S., Markham, M., Twitchen, D. J., Park, H., Lukin, M. D. and Lončar, M., "Coupling of NV centers to photonic crystal nanobeams in diamond," *Nano Lett.* 13(12), 5791-5796 (2013).
- [16] Luozhuo, L., Schroder T., Chen E. H., Walsh M., Bayn I., Goldstein J., Gaathon O., Trusheim M. E., Lu M., Mower J., Cotlet M., Markham M. L., Twitchen D. J. and Englund, D., "Coherent spin control of a nanocavity-enhanced qubit in diamond," *Nat. Commun.* 6, 6173 (2015).
- [17] Lee, J. C., Bracher, D. O., Cui, S., Ohno, K., McLellan, C. A., Zhang, X., Andrich P., Aleman B., Russell K. J., Magyar A. P., Aharonovich I., Bleszynski Jayich A.C., Awschalom D. D. and Hu, E. L., "Deterministic coupling of delta-doped nitrogen vacancy centers to a nanobeam photonic crystal cavity," *Appl. Phys. Lett.* 105, 261101 (2014).
- [18] Bracher D. O. and Hu, E. L., "Fabrication of high-Q photonic crystals in epitaxially grown 4H-SiC," *Nano Lett.* 15(9), 6202-6207 (2015).
- [19] Magyar, A. P., Lee J. C., Limarga, A. M., Aharonovich I., Rol, F., Clarke, D. R., Huang M. and Hu E. L., "Fabrication of thin, luminescent, single-crystal diamond membranes," *Appl. Phys. Lett.* 99, 081913 (2011).
- [20] Short, J. S., Osgood, R. M. and Kurtz, A. D., "Photoelectrochemical conductivity selective etch stops for SiC," *Appl. Phys. Lett.* 60, 1001 (1992).
- [21] Di Cioccio, L., Le Tiec, Y., Letertre, F., Jaussaud, C. and Bruel, M., "Silicon carbide on insulator formation using the Smart Cut process," *Electronics Lett.* 32(12), 1144-1145 (1996).
- [22] Christle, D. J., Falk, A. L., Andrich, P., Klimov, P. V., Hassan J. U., Son, N. T., Ohshima, T. and Awschalom, D. D., "Isolated electron spins in silicon carbide with millisecond coherence times," *Nat. Mat.* 14, 160-163 (2015).
- [23] Fuchs, F., Stender, B., Trupke, M., Simin D., Pflaum, J., Dyakonov V. and Astakhov G. V., "Engineering near-infrared single-photon emitters with optically active spins in ultrapure silicon carbide," *Nat. Comm.* 6, 7578 (2015).
- [24] Zhang, Y., McCutcheon, M. W., Burgess, I. B. and Loncar, M., "Ultra-high-Q TE/TM dual-polarized photonic crystal nanocavities," *Opt. Lett.* 34(17), 2694-2696 (2009).
- [25] Akahane, Y., Asano, T., Song, B. S. and Noda, S., "High-Q photonic nanocavity in a two-dimensional photonic crystal," *Nature* 425, 944-947 (2003).